CONCRETE LIBRARY OF JSCE NO. 10. DECEMBER 1987

BEHAVIOURS OF REINFORCED CONCRETE COLUMNS UNDER STATIC ALTERNATING CYCLIC LOADS

(Translation from Proceedings of JSCE, Vol.372/V-5, August 1986)

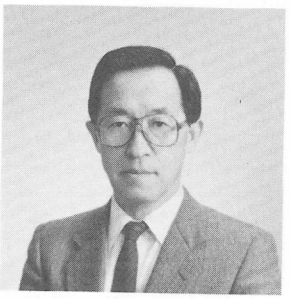

Yoshio OZAKA

Motoyuki SUZUKI

SYNOPSIS

As well as attention to stress produced in a cross section, examination of strength and deformability of members or structures is necessary to establish rational methods of designing reinforced concrete structures subject to earthquakes. This paper describes the influences of longitudinal reinforcement ratio, web reinforcement ratio and axial load on the behaviours of reinforced concrete columns with much web reinforcement under static alternating cyclic loads. In particular, the effects of these parameters on the important limit states such as flexural and diagonal crack occurrences, member yielding and ultimate state of members were investigated. As a result, the main factor influencing the above mentioned states and ductility of the columns was found to be longitudinal reinforcement. The additional displacement due to elongation of longitudinal bars extending from the footing must be taken into consideration in order to evaluate the displacement of columns beyond member yielding. Furthermore, a maximum-point-directed type model without slippage is proposed to represent the force-displacement relationship.

Yoshio OZAKA, BSc, MSc, phD Engineering, Tohoku University, SENDAI. Senior Engineer, Structures Design Office, '66 and Deputy Director, Osaka Construction Bureau, '70, Japanese National Railways; Professor of Structural Engineering, Tohoku University, since '72. MEMBERSHIPS : Delegation of Japan to CEB ; Commission "Seismic Design" of FIP; ACI; IABSE; JSCE; JCI; JPCEA. Japan Railway Eng. Ass. Meritorious Paper Award for study of PC through-girder bridge, '67; JSCE Award (Yoshida Prize) for study of quality control of field concrete, '68; JCI Award for study of cracking behavior of RC tension member under drying, '86.

Motoyuki SUZUKI is a research associate of the Department of Civil Engineering at Tohoku University, SENDAI, Japan. He received his Master of Engineering Degree in 1977 from Tohoku University. His research interests include behavior of reinforced concrete structure during earthquake, and reliability problems in reinforced concrete structure. He is a member of ACI, IABSE, JSCE, and JCI.

---

1. INTRODUCTION

Recently, many reinforced concrete viaducts are used for public structures such as railway bridges and highway bridges. Much serious damage due to flexural-shear was inflicted in the middle-height beams and columns of reinforced concrete viaducts of the Tohoku Bullet Line during the Miyagiken-oki-Earthquake (1978), and thus reexamination of the design method is needed [1]. As well as attention to stress produced in a cross section, examination of strength and deformability of members or structures is necessary to establish a rational method of designing reinforced concrete structures subject to earthquakes.

Behaviours occurring up to the ultimate state of column members have been studied mainly in the field of architecture in Japan. For example, Ikeda [2] and Yamada [3] pointed out that the influence of axial load on resistance and deformability of RC columns is significant and that the greater the number of load repetitions , the lower the stiffness and resistance of the members. Noguchi [4] and Takiguchi [5] examined the influence of bond between reinforcement and concrete on the failure mode and the nature of deformation. Kurosho [6] studied the flexural behaviours of RC columns under variable axial load. Hirosawa [7] analyzed the shear resistance of RC beams and columns. Yamada [8] analyzed the elasto-plastic flexural characteristics of RC members under constant axial load. Hattori [9], Kaneko [10] and Muguruma [11] have tried to evaluate the shear resistance of RC members on the basis of truss-analogy and shear transfer theory. Yoshioka [12] experimentally examined the influences of details of longitudinal reinforcement and tie bars on the shear resistance and performance of RC columns in order to assure large deformability. And Suenaga [13] and Shimazu [14] statistically analyzed the relation between the resistance or deformability and various other factors. The features of the above mentioned research studies are as follows: (i) shear span ratios (a/d) of the members are approximately smaller than 3, and (ii) the ratio of compressive stress due to axial load to concrete compressive strength is relatively large.

On the other hand, the a/d of columns of RC viaducts varies from about 3 to 5, which is larger than that of columns in buildings. Furthermore, axial compressive stress in a column section due to dead load is quite small,i.e., 10 $\sim$ 15 kgf/cm^2. In the field of civil engineering, some research has been done regarding this topic [15][16][17]. The features of the members studied [15][16] are as follows: (i) the amount of transverse reinforcment is quite small, and (ii) the longitudinal reinforcement bars are arranged near the edges of the compression and tension zones (called beam-type arrangement). But in many cases, the longitudinal reinforcement bars are arranged along the perimeter of the section (called column-type arrangement). The behaviour of columns with the column-type arrangement and a large amount of transverse reinforcement have not been studied so far.

The purpose of this investigation is to study the behaviours of RC columns with the column-type arrangement under static alternating cyclic load. The focus of our investigation is on the influences of longitudinal reinforcement, transverse reinforcement and axial load on the resistance, ductility and force-displacement characteristics of the columns.

2. EXPERIMENTAL PROGRAM

2.1 Material

The mix proportion of the concrete is shown in Table 1. Compressive and tensile strengths of the concrete cylinders (10 cm x 20 cm) are shown in Table 2. All the deformed bars which were used in this experiment had bamboo-type lugs. Properties of the reinforcing bars are shown in Table 3.

Table 1. Mix proportion of concrete

Max. size of coarse aggregate (mm)		25
Slump (cm)		12±2.5
Air content (%)		4±1
Water-cement ratio (%)		49
Coarse aggregate-fine aggregate ratio (%)		44
Unit weight (kg/m³)	Water W	170
	Cement C	347
	Fine Aggregate S	755
	Coarse Aggregate G	1011

Table 2. Properties of concrete

Specimen No.	1	2	3	4	5	6	7	8	9	10	11	12
Age (day)	33	24	25	31	26	35	26	37	27	27	30	31
Compressive strength (kgf/cm²)	202	329	329	338	329	347	327	351	202	329	202	202
Tensile strength (kgf/cm²)	19.2	26.5	26.9	24.7	27.3	25.7	23.4	26.2	18.5	27.8	18.8	19.0
Modulus of elasticity ($\times 10^5$kgf/cm²)	1.52	1.88	1.90	2.15	1.92	2.15	2.15	2.15	1.52	1.95	1.52	1.52

Table 3. Properties of reinforcement

Size	D 6	D10	D13	D16	D19	D25
Yield load (tonf)	1.19	2.40	4.93	7.00	10.00	20.37
Yield strain (μ)	2000	2190	2670	2480	2510	—
Tensile strength (tonf)	1.72	3.67	7.00	11.90	16.13	30.15
Elongation (%)	21.1	14.4	16.1	15.3	13.4	—

2.2 Test Specimens

Table 4 describes the 12 test columns. A typical test specimen is shown in Fig. 1. All test specimens were square, 400 mm (15.7 in) by 400 mm and 1400 mm (55.1 in) in height. Columns had a constant a/d ratio (4.0), while longitudinal reinforcement ratio (ρl), transverse reinforcement ratio (ρw) and axial compressive stress (σo) varied.

Table 4. Specimen details

Specimen No.		1	2	3	4	5	6	7	8	9	10	11	12
Longitudinal reinforcing	Size	D13	D19	D25	D19	〃	〃	〃	〃	〃	D16	〃	〃
	Ratio ρ_t(%)	0.950	2.149	3.800	2.149	〃	〃	〃	〃	〃	1.490	〃	〃
Lateral reinforcing	Size-set	D10-1	〃	〃	D6-1.5	D6-1	D10-1	D6-1.5	D10-1	〃	〃	D6-1.5	D6-1
	Spacing (cm)	10	〃	〃	〃	〃	12.5	13.3	10	〃	〃	〃	〃
	Ratio ρ_w(%)	0.357	〃	〃	0.238	0.158	0.285	0.178	0.357	〃	〃	0.238	0.158
Axial stress σ_o (kgf/cm²)		15	〃	〃	〃	〃	〃	10	40	0	15	〃	〃
Standpoint	ρ_t	○	○	○							○		
	ρ_w		○		○	○	○	○			○	○	○
	σ_o		○						○	○			

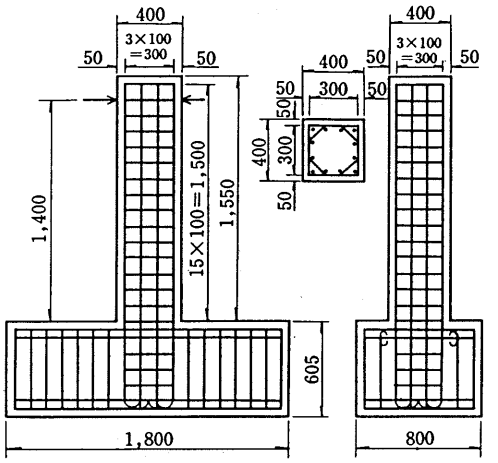

Fig. 1 Details of the specimen

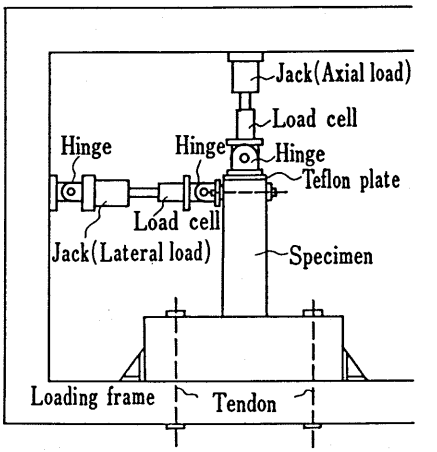

Fig. 2 Schematic view of test apparatus

The ratio of longitudinal reinforcement in columns of RC viaducts of the Tohoku Bullet Line is about 2.0% and web reinforcement ratio is about 0.08%. Axial compressive stress in column cross sections due to dead load and other factors is about 15 kgf/cm^2 and variable axial stress during earthquakes is estimated to be about ± 6 kgf/cm^2. Therefore,longitudinal reinforcement ratio varied from 0.95% to 3.8%, transverse reinforcement ratio varied from 0.158% to 0.357%, and axial compressive stress varied from 0 to 40 kgf/cm^2.

2.3 Test Arrangement and Procedure

Fig. 2 shows the test setup. After placing the specimen in the test setup and attaching all instrumentation, an axial load was applied to the column. This axial load was maintained at a constant level while the column was loaded horizontally.

Fig. 3 shows the loading schedule. A lateral load was applied with gradually increasing levels of displacement ductility factor. δc indicates the horizontal displacement at the loading point when a flexural crack occurs, and δy indicates the horizontal displacement at the same point when the member yields. A digital strain measurement instrument was used in the test.

3. CALCULATION METHOD OF DEFLECTION UNDER BENDING MOMENT

3.1 Moment-Curvature Relationship of Cross Section

Deflection of a RC column subjected to bending moment was calculated on the basis of the moment-curvature relationship (M-ϕ relationship) of a cross section. Fig. 4 shows a flow chart of the calculation. The following assumptions were made.

(1) The plain section initially remains plain at any bending stage.
(2) The stress-strain relationships of the reinforcement and the concrete are known.
(3) Tensile strength of concrete is assumed to be 70 f'c/(280+f'c) [18], and the bond slip between steel and concrete is neglected.
(4) The section is divided into a number of elements, and in each element, strain and stress are assumed to be constant. The position of the neutral

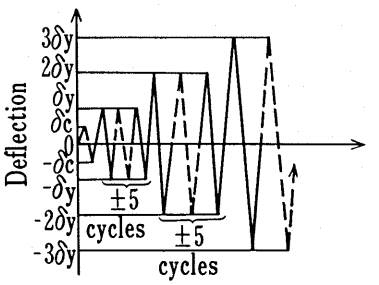

Fig. 3 Horizontal force histories

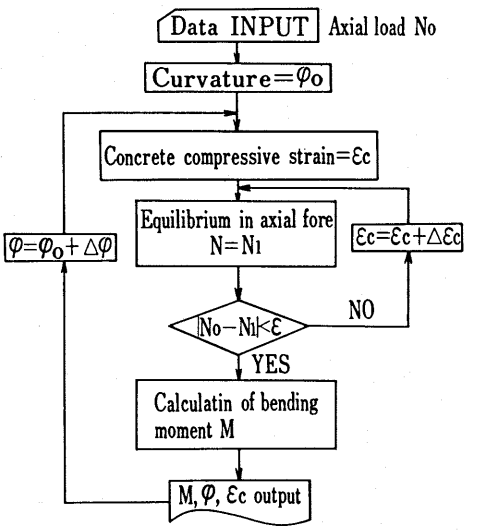

Fig. 4 Flow chart of M-ϕ relation

axis of the cross section is determined so as to fulfil the following equilibrium equations:

a. equilibrium of axial force,

$$N=\sum_{i=1}^{n} Nci+\sum_{i=1}^{n'} Nsi \qquad (1)$$

b. equilibrium of bending moment,

$$M=\sum_{i=1}^{n} Nci*li+\sum_{i=1}^{n'} Nsi*li' \qquad (2)$$

where Nci = axial force in the i-th concrete fiber,
Nsi = axial force in the i-th steel fiber,
li = the distance from the middle of the section to the i-th concrete fiber,
li' = the distance from the middle of the section to the i'-th steel fiber.

Curvature of the cross section is defined as $\phi = (\varepsilon c+\varepsilon s)/d$,
where εc = strain at extreme fiber in compression,
εs = steel strain at extreme fiber in tension.

3.2 Properties of Materials

(1) Concrete

There are several constitutive models of concrete in compression, for example the e-function method [19], the parabola-rectangle model (CEB method) [20], the ACI model [21], and so on. It is clear that the behaviour of concrete in compression depends on the confinement [22]. Confinement resulting from the presence of transverse reinforcement increases the strength, and more significantly, the strain capacity of concrete in compression. An increase in confinement also results in a flatter descending branch of the concrete compressive stress-strain diagram. Therefore, the stress-strain model of concrete presented in ACI regulations is adopted a basis of for calculating in this study (cf. Fig.5).

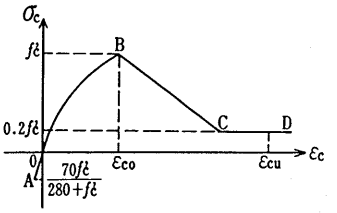

fc : compressive strength, εcu : ultimate strain
p' : stirrup volumetric ratio,
b' : length of shorter side of stirrup,
s : spacing of stirrup,

$OA: \sigma_c = \frac{2f'_c}{\varepsilon_{co}}\varepsilon_c$

$OB: \sigma_c = f'_c\left[\frac{2\varepsilon_c}{\varepsilon_{co}} - \left(\frac{\varepsilon_c}{\varepsilon_{co}}\right)^2\right]$

$BC: \sigma_c = f'_c\left[1 - \frac{0.5(\varepsilon_c - \varepsilon_{co})}{\varepsilon_{50h} + \varepsilon_{50u} - \varepsilon_{co}}\right]$

$\varepsilon_{50h} = \frac{3}{4}p'\sqrt{b'/s}$

$\varepsilon_{50u} = \frac{0.21 + 0.002f'_c}{f'_c - 70}$

$CD: \sigma_c = 0.2f'_c$

Fig. 5 Stress-strain relationship of concrete

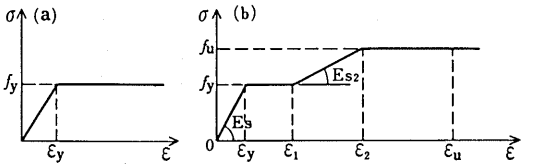

Fig.6 Stress-strain relationship of reinforcement

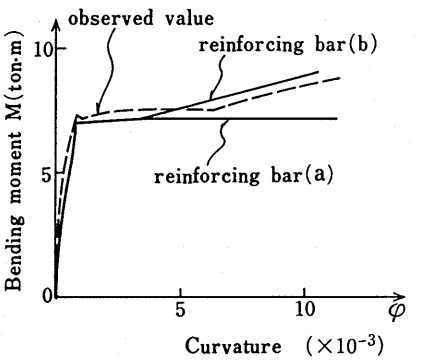

Fig. 7 Comparison of M-ϕ relationship

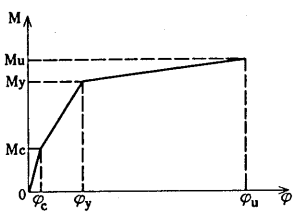

Fig. 8 M-ϕ relationship

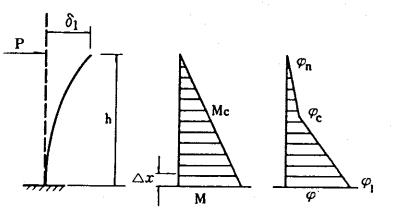

Fig. 9 Displacement δ1

(2) Reinforcement

The following two constitutive models of reinforcing bars were assumed: (1) a model without strain hardening (Fig.6(a)),and (2) a model with strain hardening (Fig.6(b)). The theoretical M-ϕ relations on the basis of these two models were compared with available test results for reinforced concrete beams under flexure (Fig.7). This figure shows that the analytical approach used with reinforcing bars(b) can closely predict the measured curve. Therefore, a stress-strain curve with strain hardening was used in this study. The following values were determined by tension testing of reinforcing bars: ε_1 = 15000μ, ε_2 = 60000μ, εu = 100000μ, Es = 1.9×10^6 kgf/cm^2, fy = strength at yielding, and fu = tensile strength.

(3) Calculation of Flexural Deflection

The ideal moment-curvature curve is shown in Fig. 8. The curve consists of three lines connecting limit states such as the occurrence of a flexural crack, member yielding, and ultimate state. Then the horizontal displacement δ1 due to

bending moment at the loading point of the column is calculated by the following equation (c.f. Fig.9).

$$\delta 1=\sum_{i=1}^{n}\phi i(\Delta x)^2/2+\sum_{i=1}^{n-1}\left(\sum_{k=1}^{i}\phi k\right)(\Delta x)^2 \qquad (3)$$

In this research, n = 14.

(4) Additional Displacement due to the Elongation of Bars from the Footing.

It has been pointed out that the additional deflection resulting from the rotation of the column due to the elongation of longitudinal bars extending from the footing must be taken into account when calculating horizontal deflection of the column [15][23]. The additional deflection is found based on the following procedure and assumptions.

1. The strain distribution of the bars embedded in the footing is assumed to be triangular (cf. Fig.10 (a)).
2. The distance 1 between the surface of the footing and the position of the bar strain of 0 is estimated by the following equations. Eq. (4) indicates the relationship between average bond stress τc and strain εs of the reinforcing bars (Fig.10 (b)).

$$\tau c = f(\varepsilon s) = 0.84\sqrt{\varepsilon s} \qquad (4)$$

$$\sigma t*\pi r^2 = 2\pi r\int_0^1 f(\varepsilon s)dx = 2\pi r\int_0^1 f(\varepsilon s/1*(1-x))dx \qquad (5)$$

3. Additional horizontal displacement $\delta 2$ at the loading point can be calculated by the following equations:

$$\Delta = 1*\varepsilon so/2, \quad \theta = \Delta/x = 1*\varepsilon so/2*x \qquad (6)$$

$$\delta 2 = h*\theta = h*1*\varepsilon so/2*x \qquad (7)$$

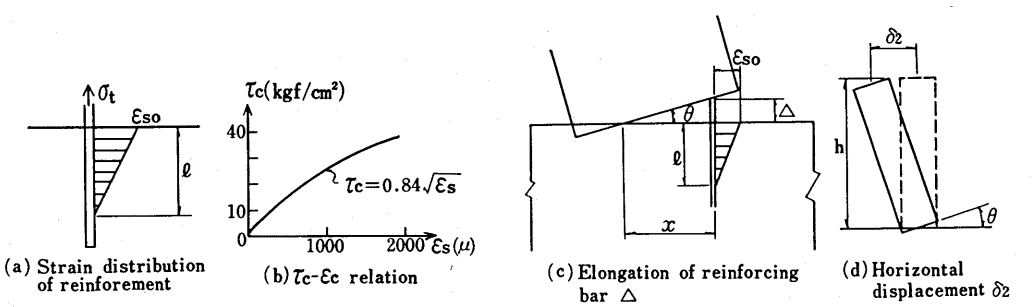

(a) Strain distribution of reinforement (b) τc-εc relation (c) Elongation of reinforcing bar Δ (d) Horizontal displacement $\delta 2$

Fig. 10 Displacement $\delta 2$

4. EXPERIMENTAL RESULTS AND CONSIDERATIONS

4.1 Influences of Principal Parameters on Behaviour of Members

Table 5 shows the test results. Member yielding is identified as the yield of longitudinal bars near the tension edge. "Limit displacement" means the displacement of the state at which the load applied to the specimen is equal to the member yielding load in the descending branch of the P-δ curve. In table 5 load is the horizontal load applied to the specimen, and displacement is the

Table 5. Test results

Specimen No.	Flexural crack		Diagonal crack		Member yield		Maximum load		δmax	Pmax/Py	Ductility	
	Pc	δc	Ps	δs	Py	δy	Pmax	δu			δu/δy	δmax/δy
1	5.32 −2.89	1.2 −0.9	8.56 − 7.06	4.2 − 3.8	10.77 −10.13	6.9 − 7.1	13.20	42.5	56.4	1.23	6.2	8.2
2	4.02 −3.90	0.7 −1.1	15.91 −14.12	8.1 −10.1	−18.30 −14.67	11.0 −11.0	20.73	33.5	44.5	1.13	3.0	4.0
3	3.04 −3.00	0.7 −0.7	17.97 −19.67	8.1 −11.5	24.24 −23.24	13.0 −14.0	28.12	26.2	65.3	1.16	2.0	5.0
4	6.36 −4.03	1.8 −1.1			18.63 −16.89	11.0 −11.6	23.57	33.4	55.3	1.27	3.0	5.0
5	1.56 −1.36	0.1 −0.5	16.83 −11.82	9.1 − 6.2	18.50 −16.62	11.0 −10.9	21.24	34.1	43.8	1.15	3.1	4.0
6	4.81 −4.33	1.3 −1.1			17.63	10.5	21.20	41.9	52.7	1.20	4.0	5.0
7	2.98 −2.08	0.4 −0.3	15.60	9.6	16.59	10.4	23.42	31.7	52.9	1.41	3.0	5.1
8	4.92 −3.42	0.9 −0.8	17.22 −17.51	7.0 − 7.9	21.12 −20.09	10.5 −10.5	25.72	21.1	52.7	1.22	2.0	5.0
9	4.00 −2.79	1.6 −1.1	10.93 −11.38	8.0 − 7.8	12.33 −13.47	10.0 −10.0	14.78	20.5	59.9	1.20	2.0	6.0
10	1.95 −2.53	0.4 −0.7	11.32 −12.55	6.0 − 8.9	13.79 −13.20	9.0 − 9.5	16.37	27.4	45.3	1.19	3.0	5.0
11	3.84 −4.02	0.7 −1.1	10.77 − 9.27	5.9 − 4.0	12.96 −13.89	9.1 − 8.1	15.66	27.3	54.7	1.21	3.0	6.0
12	3.88 −2.89	0.7 −0.7	10.56 −11.94	4.4 − 8.0	15.42	9.0	18.51	27.4	54.0	1.20	3.0	6.0

Unit : Pc, Ps, Py, Pmax : tonf,δc,δs,δy,δu, δmax : mm,

horizontal displacement at the loading point.

(1) Flexural Crack

Table 6 shows comparisons between test results and analysis at the occurrence of a flexural crack. Analytical values 1 were calculated on the basis of the M–φ relationship. Analytical values 2 were based on the following equation [25]:

$$Mc2 = 1.8\sqrt{Fc}\cdot Ze + N\cdot d/6 \qquad (8)$$

where Fc = concrete compressive strength (kgf/cm^2), Ze = section modulus, and N = axial force (kgf).

The mean value m of the ratio Mc/Mc1 was 0.944, and the standard deviation σ is 0.362; for the ratio Mc/Mc2, m = 1.02, and σ = 0.414. Considerable variabilities were caused by the method of confirmation of the occurrences of flexural cracks. In fact, strains of the longitudinal bars at the boundary between the footing and the column were scattered considerably [see Fig. 11]. Only for specimens with longitudinal strain of about 100μ at the occurrence of flexural cracks, m = 0.85, σ = 0.151 for Mc/Mc1, m = 0.91, σ = 0.191 for Mc/Mc2, and m = 1.37, σ = 0.73 for δc/δc1.

(2) Diagonal Cracks

Table 6. Flexural crack

Specimen No.	Measured value Mc (t·m)	Measured value δc (mm)	Calculated value ① Mc1 (t·m)	Calculated value ① δc1 (mm)	Mc / Mc1	δc / δc1	Calculated value ② Mc2 (t·m)	Mc / Mc2
1	7.45	1.2	4.99	0.78	1.49	1.53	4.59	1.62
2	5.63	0.7	6.22	0.51	0.91	1.37	5.83	0.97
3	4.26	0.7	6.76	0.51	0.63	1.37	6.40	0.67
4	8.88	1.8	6.26	0.58	1.42	3.10	5.89	1.51
5	2.18	0.1	6.22	0.51	0.35	0.20	5.83	0.37
6	6.73	1.3	6.30	0.58	1.07	2.24	5.96	1.13
7	4.17	0.4	5.68	0.64	0.73	0.63	5.82	0.72
8	6.89	0.9	8.90	0.71	0.77	1.27	8.48	0.81
9	5.60	1.6	3.90	0.78	1.44	2.05	3.31	1.69
10	2.73	0.4	6.01	0.52	0.45	0.77	5.60	0.49
11	5.38	0.7	5.22	0.72	1.03	0.97	4.73	1.14
12	5.43	0.7	5.22	0.72	1.04	0.97	4.73	1.15

Table 7. Diagonal crack

Specimen No.	Measured value Ps (ton)	Calculated value (tonf) Ps1	Ps2	Ps3	Measured/Calculated Ps/Ps1	Ps/Ps2	Ps/Ps3
1	8.56	9.02	4.68	8.31	0.95	1.83	1.03
2	15.91	10.88	5.73	14.60	1.46	2.78	1.09
3	17.97	11.95	5.73	18.86	1.50	3.14	0.95
4	–	11.63	5.79	14.86	–	–	–
5	16.83	11.49	5.73	14.60	1.46	2.94	1.15
6	–	11.80	5.86	15.13	–	–	–
7	15.60	11.46	5.40	14.54	1.36	2.89	1.07
8	17.22	13.87	7.24	15.24	1.24	2.34	1.13
9	10.93	7.97	3.71	10.55	1.37	2.95	1.04
10	11.32	11.30	5.73	12.89	1.00	1.98	0.88
11	10.77	9.14	4.68	9.31	1.18	2.30	1.15
12	10.56	9.14	4.68	9.31	1.15	2.26	1.13

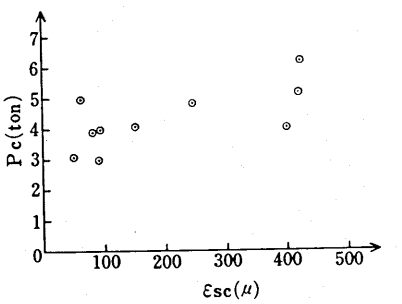

Fig. 11 Relationship between Pc and strain of longitudinal bar

Table 7 shows comparisons between test results and analysis at the occurrence of diagonal cracks. Psl and Ps2 were calculated by the following equations proposed by the RC Committee of the Japan Architectural Center:

$$Psl = 0.265 \cdot b \cdot d \sqrt{Fc} + Mbc/(M/Q - d/2) \quad (9)$$

where Mbc = member strength at the occurrence of a flexural crack (Mbc = Mcl),
M = bending moment, Q = shear force.

$$Ps2 = 0.163\ (4.04 - M/Q \cdot d) \sqrt{cFt(cFt + \sigma o)} \cdot b \cdot d \quad (10)$$

where cFt = concrete tensile strength (=1.8 $\sqrt{Fc}$),
σo = axial compressive stress.

Psl represents the member strength at the beginning stage of development from flexural cracks into diagonal cracks, and Ps2 corresponds to "shear-tension crack strength." The calculated values Psl in comparison with Ps2 almost entirely agreed with the experimental values.

The calculated values Ps3 are based on the following CEB equation [20]:

$$Ps3 = 0.25 fctd \cdot K(1 + 50Pt) \cdot b \cdot d \quad (11)$$

where K = 1.6-d ≧ 0, fctd = concrete tensile strength, Pt = the ratio of tension bars. Under axial force the values obtained by equation (11) are multiplied by

(1+Mo/Md) (where Md is applied bending moment, Mo is bending moment at which extreme fiber stress of the section is 0). The calculated values based on equation (11) were in good agreement with the observed values. In fact, mean value and standard deviation were 1.06 and 0.085, respectively.

Fig. 12 shows the relationships between member strength at the occurrence of diagonal cracks and parameters. The relation between Ps and longitudinal reinforcement ratio is approximately linear ($Ps = 12.91 + 0.25\rho l$, coefficient of correlation is 0.928). And as axial compressive stress increases, the load Ps increases. But no influence of the amount of tie bars on Ps was recognized.

(3) Member Yielding

Table 8 shows comparisons between test results and analysis at member yielding. Bending moment Myl in the critical section, horizontal displacement $\delta y1$ at the loading point due to flexure, and additional horizontal displacement $\delta y2$ due to elongation of longitudinal bars from the footing were calculated by the method mentioned in section 3. The mean value m and standard deviation σ were 1.18, 0.12 for My/Myl and 1.84, 0.19 for $\delta y/\delta y1$, respectively. But for the ratio of δy to $(\delta y1 + \delta y2)$, its mean value m = 0.988, standard deviation σ = 0.06. Therefore, the displacement of the column at member yielding can be estimated by the displacement due to flexure plus additional displacement due to the elongation of longitudinal bars. Fig. 13 shows the relation between Py and several parameters. The relations between Py and longitudinal reinforcement ratio or axial compressive were approximately linear as follows:

$$Py = 8.0 + 3.95\rho l \quad \text{(coefficient of correlation 0.968)} \qquad (12)$$

$$Py = 14.18 + 0.2\sigma o \quad \text{(coefficient of correlation 0.904)} \qquad (13)$$

But the effect of web reinforcement ratio on Py was negligible.

(4) Ultimate state

Table 9 shows comparisons between test results and analysis at ultimate state. Maximum bending moments Mmaxl and the displacements δuo at that time were calculated on the basis of the above mentioned M-ϕ relationship. δuo is obtained as the sum of the displacement due to flexure δul and twice the additional displacement $\delta u2$ due to elongation of the longitudinal bars. For the ratio of observed value Mmax to calculated value Mmaxl, the mean value m and standard deviation σ were 1.13 and 0.138, respectively. As for $\delta u/\delta uo$, m = 0.996 and σ = 0.284. Therefore, the displacement at the maximum load for a column with "column type" longitudinal bar arrangement can be estimated by the sum of the displacement due to flexure and the twice the displacement due to the elongation of longitudinal bars. This method of evaluation was derived from the "beam type" column arrangement [23]. One of the main reasons why the displacement of twice $\delta u2$ must be added is the fact that the loss of bond between bar and concrete, especially beyond member yielding under cyclic loading, is remarkable as compared with the case under monotonic loading or before member yielding. The main factors influencing Pmax were longitudinal reinforcement ratio and axial compressive stress (Fig. 14). The following relationships were obtained between Pmax and ρl or σo.

$$Pmax = 8.69 + 5.2\ \rho l, \quad \text{(coefficient of correlation: 0.996)} \qquad (14)$$

$$P_{max} = 17.5 + 0.23\,\sigma_o, \quad \text{(coefficient of correlation: 0.820)} \qquad (15)$$

Table 8. Member yielding

Specimen No.	Measured value My (t·m)	Measured value δ_y (mm)	Calculated value M_{y1} (t·m)	Calculated value δ_{y1} (mm)	Calculated value $\delta_{y1}+\delta_{y2}$ (mm)	Measured/Calculated My / M_{y1}	Measured/Calculated δ_y / δ_{y1}	Measured/Calculated δ_y / $\delta_{y1}+\delta_{y2}$	$\frac{\delta_{y2}}{\delta_{y1}+\delta_{y2}}$ (%)
1	15.08	6.9	11.14	4.91	8.04	1.35	1.41	0.86	38.9
2	25.62	11.0	21.61	5.55	10.51	1.19	1.98	1.05	47.2
3	33.94	13.0	33.15	5.91	12.65	1.02	2.20	1.03	53.3
4	26.08	11.0	21.64	5.51	10.45	1.20	2.00	1.05	47.3
5	25.90	11.0	21.61	5.55	10.51	1.20	1.98	1.05	47.3
6	24.68	10.5	21.71	5.49	10.40	1.14	1.91	1.01	47.3
7	23.23	10.4	20.57	5.55	10.43	1.13	1.87	1.00	46.8
8	29.57	10.5	26.72	5.54	10.93	1.11	1.89	0.96	49.3
9	17.26	10.0	17.68	5.99	11.03	0.98	1.67	0.91	45.7
10	19.31	9.0	15.92	4.87	8.61	1.21	1.85	1.05	43.4
11	18.14	9.1	15.17	5.41	9.51	1.20	1.68	0.96	43.2
12	21.59	9.0	15.17	5.41	9.51	1.42	1.66	0.95	43.2

δ_{y1}: displacement due to flexure
δ_{y2}: displacement due to elongation of longitudinal bar

Table 9. Ultimate state

Specimen No.	Measured value Mmax (t·m)	Measured value δ_u (mm)	Calculated value M_{max1} (t·m)	Calculated value δ_{uo} (mm)	Measured/Calculated Mmax / M_{max1}	Measured/Calculated δ_u / δ_{uo}	$\frac{\delta_{u2}}{\delta_{uo}}$ (%)
1	18.48	42.5	13.74	24.44	1.34	1.74	58
2	28.29	33.4	27.27	32.85	1.04	1.02	67
3	39.37	26.2	42.68	37.63	0.92	0.70	69
4	33.00	33.4	27.32	32.89	1.21	1.02	67
5	29.74	34.1	27.26	32.89	1.09	1.04	67
6	29.68	41.9	27.38	33.00	1.08	1.27	68
7	32.79	31.7	26.06	33.20	1.26	0.95	67
8	36.01	21.1	33.12	31.38	1.09	0.67	62
9	20.69	20.5	22.84	32.69	0.91	0.63	65
10	22.92	27.4	19.93	29.11	1.15	0.94	65
11	21.92	27.3	19.06	27.62	1.15	0.99	61
12	25.91	27.4	19.06	27.60	1.36	0.99	61

$\delta_{uo} = \delta_{u1} + 2\delta_{u2}$
δ_{u1} : displacement due to flexure at the maximun load
δ_{u2} : displacement due to elongation of longitudinal bar

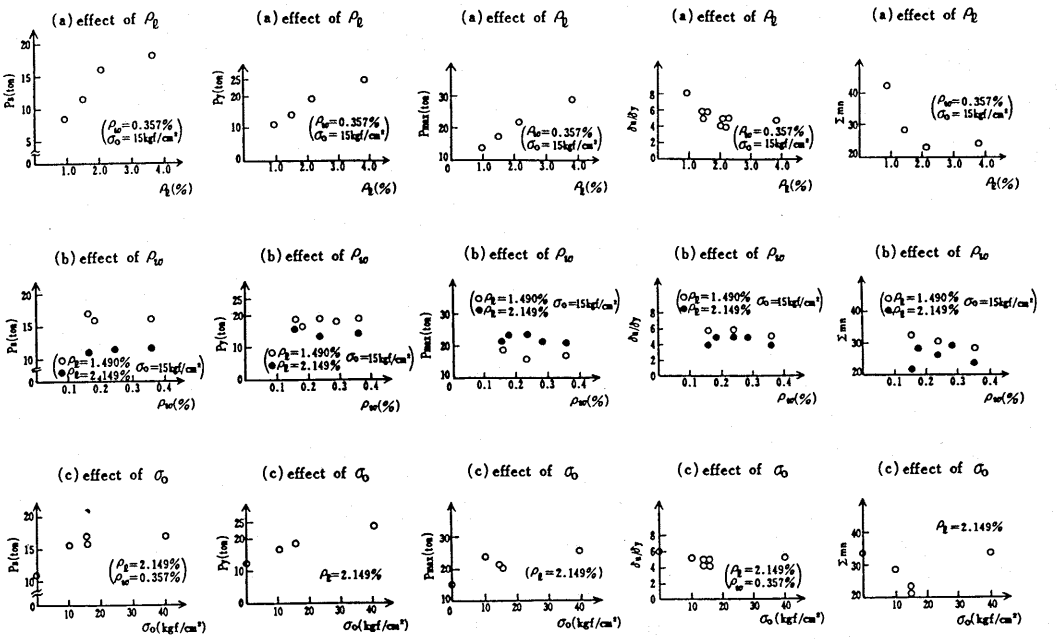

Fig. 12 Ps Fig.13 Py Fig.14 Pmax Fig.15 δu/δy Fig.16 Σm_n

(5) Rotation of Column due to Elongation of Longitudinal Bars

It is generally said that the influence of the elongation of longitudinal bars extending from the footing on the horizontal displacement of the column is significant. Therefore, two dial gauges were set up at a height of 220 mm from the footing to measure the elongation of longitudinal bars (see Fig. 17). The

average of two measurements, ℓ1 and ℓ2, was regarded as representing the elongation of the bars. Residual elongation at a load of 0 during the displacement level of 1-δy was slight, but the elongation increased gradually beyond the level of 2δy . Rotation of column due to the elongation of longitudinal bars is calculated by θ = (ℓ1-ℓ2)/ℓo, (ℓo = the distance between two measurement points). Fig. 17 shows the ratio of the displacement due to rotation (δR = h*θ) to the total horizontal displacement (δ). It is seen that the ratio of δR /δ at 3δy loading reaches about 0.8 although the ratio is about 0.5 ∿ 0.6 at 1-δy loading. The ratios δy2/(δy1+δy2) obtained from the calculated values δy1 and δy2 were 0.46 at 1δy loading and 0.65 at 3δy loading on the average. The main reason why the ratios δR/δ obtained in this experiment were bigger than the calculated ratios was due to the fact that elongation of bars between the surface of the footing and the measurement points was measured in addition to elongation of the bars from the footing since the points at which elongation of bars was measured were located 220 mm in height above the footing.

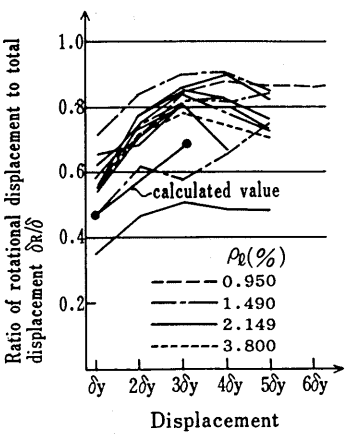

Fig. 17 Elongation of longitudinal bars

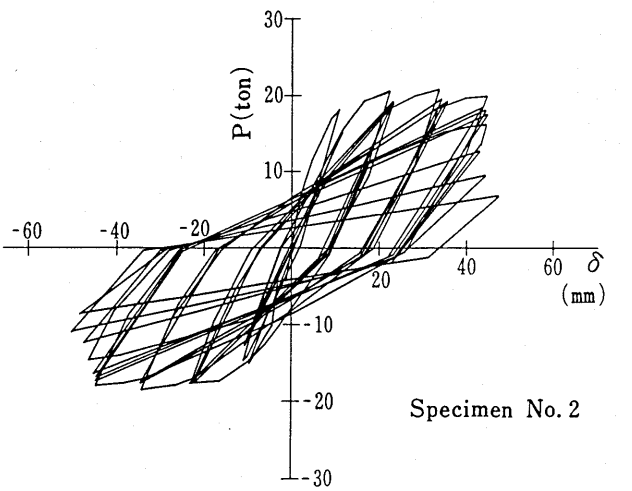

Fig. 18 Example of force-displacement curve

4.2 Force-Displacement Curves

(1) P-δ curves

Fig. 18 shows the force-displacement hysteresis loops (P-δ curve) at 1 and 5 cycles in specimen No. 2. P-δ curves for other specimens indicate almost the same spindle-shape as specimen No. 2 up to the ultimate state in spite of variable factors. In this experiment, the influences of longitudinal bars, web reinforcements and axial compressive stress on the shape and area of the loops were negligible.

(2) Model of Envelope of P-δ Curves

In order to model the P-δ curves of RC members subjected to cyclic loading, parameters which influence the envelope of P-δ curves must be clarified. Fig. 19 shows the nondimensional envelopes of P-δ curves. Judging from Fig. 19(a), it is known that the influence of longitudinal reinforcement ratio on the

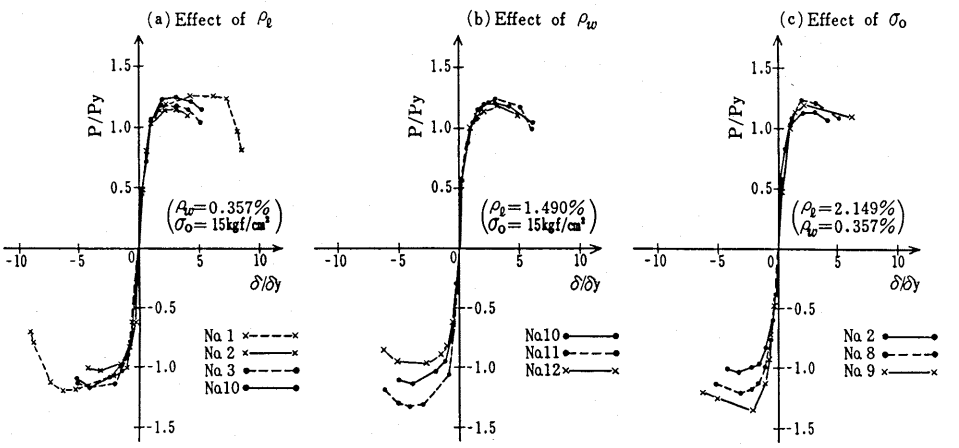

Fig. 19 Nondimensional envelopes of P-δ curves

behavior of a column beyond member yielding is significant. In fact the smaller the longitudinal reinforcement ratio is, the larger the ratio Pmax/Py and the higher the deformability. In case of ρl = 0.95% and 3.80%, Pmax/Py became 1.22 and 1.11, respectively, and δmax/δy became about 7.8 and 5.0, respectively. Furthermore, judging from Fig. 19(b) and (c) the effects of web reinforcement ratio and axial compressive stress on the envelope curves of P-δ curves were not significant.

(3) Model of P-δ Hysteresis Loop

In order to model the P-δ curves for the analysis, hysteresis loops as well as skeletons of P-δ curves must be modeled rationally. The loops are considerably influenced by dimension, arrangement of reinforcement, loading pattern and so on. Several analytical models of P-δ curves have been proposed, for example, by Clough [27], Kanno and Fukada [28], Takeda, [29] and others. Although it is very difficult to propose a model of the P-δ curve due to its having only 12 columns, the following model could be proposed within this experiment.

The skeleton curve can be idealized by three lines (Fig. 20). The first line expresses the perfect elastic state up to the occurrence of flexural cracks, the second one expresses the state until member yielding, and the third one is the line after member yielding, passing through the maximum point of the load. The load Pc and the displacement δc at the occurrence of flexural cracks, the load Py at member yielding, and the maximum load (resistance) Pmax can be evaluated by the above mentioned method. The displacements δy at the member yielding and δuo at the ultimate state can be obtained by consideration of the additional displacement due to elongation of bars besides theoretical displacement due to flexure. Based on the experimental results,the inclination of the third line of the skeleton curve was assumed to be 1/10 of stiffness up to member yielding from the original point.

P-δ hysteresis loops were idealized by four lines as shown in Fig. 20. The relationship between two stiffnesses Kμ(during unloading) and Ko (initial stiffness up to the member yielding) and ductility μ was obtained as followed:

$$K\mu = Ko/\mu^{0.4} \qquad (16)$$

Fig. 21 shows the relationship between Kμ/Ko and μ. After all, P-δ curves were

modeled as described above within these experimental variables.

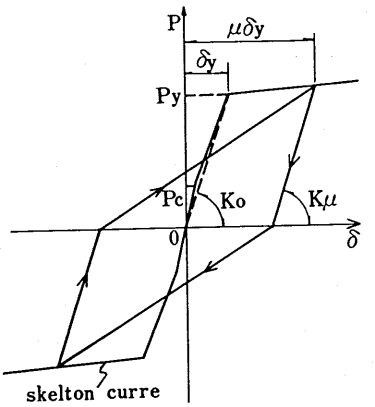

Fig. 20 Model of P-δ curve

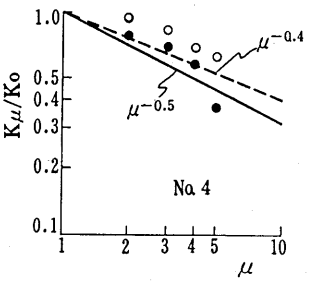

Fig. 21 Relationship between Kμ/Ko and μ

4.3 Aseismic Performance of RC Columns

(1) Ductility

Table 5 shows two ductilities, δu/δy and δmax/δy. In each ductility, significant differences were not recognized regardless of variable parameters. The main reasons were considered to be as follows:(1) since the shear span ratios of all columns were the same (4.0), behaviors of columns were remarkably affected by flexure, and (2) the web reinforcement ratio was at least 0.158%. Fig. 15 shows the influences of several parameters on the ductility δu/δy. Although the amount of web reinforcement had little effect on the ductility, the higher the ratio of the longitudinal bars is, the lower the ductility hyperbolically .

The number of repetitions of load was not taken into consideration in the evaluation of ductility such as δu/δy or δmax/δy. Then a new measure of ductility, Σm_n (m_n : the number of repetitions at nδy-loading), was introduced. Fig. 16 shows the influences of several factors on this ductility. The ductility decreases linearly or hyperbolically with increasing the longitudinal reinforcement ratio and axial compressive stress.

(2) Equivalent Viscous Damping (he)

Fig. 22 shows the influences of several factors on equivalent viscous damping (he) obtained from the fifth cycle of P-δ curves. Equivalent viscous damping (he) increases with the ratio of longitudinal bars. The influences of the amount of web reinforcement and axial compressive stress were not significant. Equivalent viscous damping (he) was about 0.1 at the 1δy loading level, about 0.4 at the 4δy loading level, and the value changed approximately linearly at the intermediate stage.

4.4 Cracking Patterns

Fig. 23 shows the cracking patterns of all columns at ultimate state. The length of plastic hinge(lp) and the real condition of longitudinal cracks are

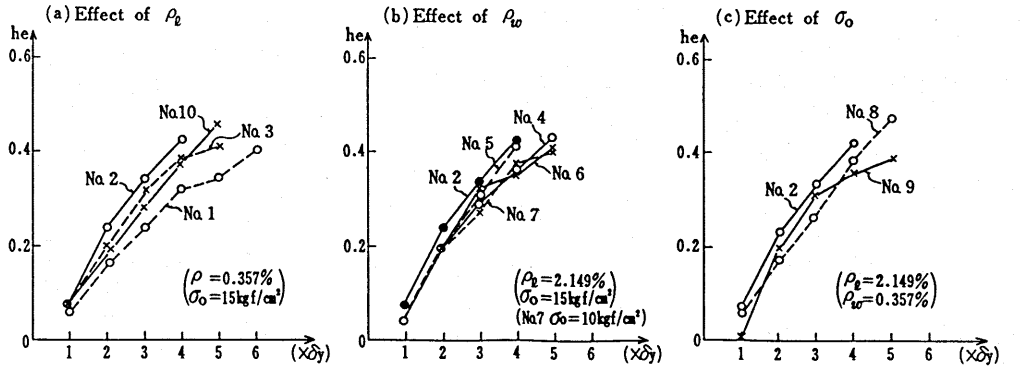

Fig. 22 Effects of parameters on he

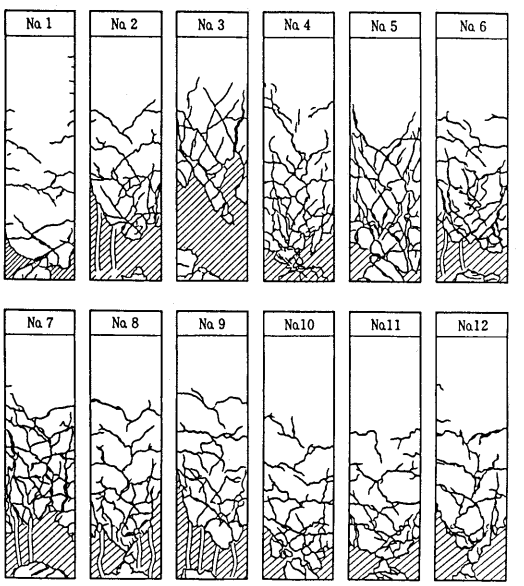

Fig. 23 Cracking patterns

Table 10 Relationship between failure condition and parameters

Constant condition	Variable		No.	Length of plastic hinje	Occurrence of longitudinal crack
ρ_ℓ=2.149% ρ_w=0.357%	σ_0 (kg/cm²)	0	9	d/2	△
		40	8	d/2	△
ρ_ℓ=1.490% σ_0=15kgf/cm²	ρ_w (%)	0.158	12	d/2	△
		0.238	11	d/2	△
		0.357	10	d/2	△
ρ_ℓ=2.149% σ_0=15kgf/cm² (No.7. σ_0=10kgf/cm²)	ρ_w (%)	0.158	5	less d/2	◎
		0.178	7	d/2	◎
		0.238	4	d/2	○
		0.285	6	d/2	○
ρ_w=0.357% σ_0=15kgf/cm²	ρ_ℓ (%)	0.950	1	less d/2	×
		1.490	10	d/2	△
		2.149	2	d/2～d	△
		3.800	3	more d	○

× : no, △ : few, ○ : yes, ◎ : remarkable

indicated in Table 10. The main factors which influence on lp and the occurrence of longitudinal cracks were longitudinal reinforcement ratio and web reinforcement ratio. Judging from cracking of columns No. 8 and No. 9, the situation of cracking was only slightly affected by axial compressive stress. The length of plastic hinge zone lp was estimated to be about d/2 (d:effective depth). Generally the higher the ratios of longitudinal bars and web reinforcements, the longer the lp.

For the columns with longitudinal reinforcement ratio of 2.149%, longitudinal cracks were apt to occur in case of the lower web reinforcement ratio; actually, the development of longitudinal cracks were remarkable in columns with web reinforcement of less than 0.18%. Thus web reinforcement is efficient in preventing the occurrence and development of longitudinal cracks. But a higher web reinforcement ratio would not necessarily prevent the occurrence of longitudinal cracks. Actually in columns with web reinforcement of 0.357%, longitudinal cracks occurred with the increasing ratio of longitudinal bars. This phenomenon was due to the fact that since the higher the web reinforcement ratio was, the greater the confinement effect of core concrete. Thus, members

would not fail in flexural compression, and longitudinal cracks were liable to occur because the higher the longitudinal reinforcement ratio is, the higher the tension stress around the tension bar. In limit state design of RC members, the occurrence of longitudinal cracks is not expected since it will cause brittle failure. In order to prevent the occurrence of longitudinal cracks, the rational combination of longitudinal reinforcement ratio and web reinforcement ratio must be considered.

5. CONCLUSIONS

From the experimental study reported in this paper, the following conclusions can be drawn:

(1) The load and the displacement at the occurrence of flexural cracks can be estimated based on the moment-curvature relationship of the column cross section assuming that the crack occurs at the longitudinal bar strain of about 100μ.

(2) The load at the occurrence of diagonal cracks can be estimated from the shear resistance equation of members without stirrups by CEB. Half of the longitudinal bars are used as tension bars.

(3) The displacement at member yielding can be estimated as the sum of additional displacement due to elongation of longitudinal bars and the flexural displacement. Displacement at ultimate state can be estimated as the sum of twice the additional displacement due to elongation of longitudinal bars and the flexural displacement.

(4) The relationship between the loads at the occcurrence of diagonal cracks, or member yielding loads or maximum loads and the ratio of longitudinal bar or the axial compressive stress were approximately linear.

(5) The ratios of the displacement due to elongation of longitudinal bars to total horizontal displacement were about 46% at a loading level of 1δy and about 65% at 3δy .

(6) The hysteresis loops of all columns were spindle-shaped up to the ultimate state. A maximum-point-directed type model without slippage represents the force-displacement relationship.

(7) The main factor influencing the ductility was the ratio of longitudinal bars. The higher the longitudinal reinforcement ratio, the lower the ductility.

(8) The main factor influencing the equivalent viscous damping(he) was longitudinal reinforcement ratio; he was about 0.1 at the loading level of 1δy and about 0.4 at 4δy.

(9) The length of plastic hinge, and the occurrence and development of longitudinal cracks depend on the combination of longitudinal reinforcement ratio and web reinforcement ratio.

As mentioned above, the main factor influencing the behaviors of columns with a relative high ratio of web reinforcement and a/d=4 is the ratio of longitudinal bars.

REFERENCES

[1] JNR Sendai Shinkansen Construction Bureau : Senkanko '78 Miyagiken-oki Earthquake Special Issue, December 1979.
[2] Akio Ikeda : Behaviors of Reinforced Concrete Columns Subjected to Axial Force, Bending Moment and Shear Force, Transactions of AIJ, No.83, pp.23-30, March 1963.
[3] Minoru Yamada and Hiroshi Kawamura : Elasto-Plastic Behaviors of Reinforced Concrete Members under Axial Force and Bending Moment, Transactions of AIJ, No.223, pp.17-25, Sept. 1974.
[4] Hiroshi Noguchi : Study on Mechanical Behavior of Reinforced Concrete Columns, Transactions of AIJ, No.234, pp.23-33, Aug. 1975.
[5] Katsumi Takiguchi : Deforming Characteristics of RC Members with and without Bond, Transactions of AIJ, No.262, pp.53-59, Dec. 1977.
[6] Shizuo Hayashi and Seiji Kokusho : Study of the Bending Behaviour of Reinforced Concrete Columns under Changing Axial Force, Transactions of AIJ, No.312, pp.28-34, Feb. 1982.
[7] Masaya Hirosawa : Strength and Ductility of Reinforced Concrete Members, Building Research Institute, Ministry of Construction, Report of the Building Research Institute, No.76, March 1977.
[8] Minoru Yamada and Hiroshi Kawamura : Elasto-Plastic Behaviours of Reinforced Concrete Members under Axial load and Bending Moment, Transaction of AIJ, No.136, pp.15-21, June 1967.
[9] Takashige Hattori, Takuji Shibata and Kazuo Ohno : Considerations on the Shear-Resistance Mechanism of Reinforced Concrete Members, Transactions of AIJ, No.200, pp.35-44, Oct. 1972.
[10] Yutaro Kaneko and Yasuo Tanaka : Shear Strength of Reinforced Concrete Short Columns, Transactions of AIJ, No.287, pp.27-38, Jan. 1980.
[11] Hiroshi Muguruma and Fumio Watanabe : Study on Shear Mechanisms in R/C Short Columns, Transactions of AIJ, No.332, pp.57-65, Oct. 1983.
[12] Kenzoh Yoshioka, Tuneo Okada and Toshikazu Takeda : Study on Impruvement of Earthquake-Resistant Behaviors of Reinforced Concrete Column, Transactions of AIJ, No.324, pp.54-62, Feb. 1983.
[13] Yasumi Suenaga and Rintaro Ishimaru : Dynanamic Analysis of Concrete Members under Combined Stress, Transactions of AIJ, No.221, pp.9-16, July 1974.
[14] Takayuki Shimazu : On the Ultimate Values of Deformation Angle for Reinforced Concrete Columns, Transactions of AIJ, No.312, pp.18-27, Feb. 1982.
[15] Minoru Ohta : An Experimental Study on the Behavior of Reinforced Concrete Bridge Piers under Cyclic Loadings, Proceedings of JSCE, No.292, pp.65-74, Dec. 1979.
[16] Taisuke Akimoto : Basic Experiments on Resistance of Reinforced Concrete Piers subjected to Cyclic High Stress, The Report pf Annual Meetings (29th, 31th and 33th).
[17] Masaharu Hirashima and Naotaka Kawaguchi : Design of Reinforced Concrete Members subject to Combined Axial Tension and Bending, Proceedings of JSCE, No.283, pp.105-116, March 1979.
[18] Park, R., Kent, D. C. and Sampson, R.A. : Reinforced Concrete Members with Cyclic Loading, Proc. of ASCE,ST7, July 1972.
[19] Kai Umemura : Plastic Deformation and Ultimate Strength of Reinforced Concrete Beams, Transactions of AIJ, No.42,Feb. 1951.
[20] CEB BULLETIN D'INFORMATION No.124/125-E, Avril 1978.
[21] ACI : Building Code Requirements for Reinforced Concrete (ACI 318-83).
[22] Hognestad, E. : A Study of Combined Bending and Axial Load in Reinforced Concrete Members, Bulletin No.399, Univ. of Illinois Engineering Experiment Station, Nov.1951.
[23] Yoshio Ozaka, Tsutomu Yanagida, Minoru Ohta and Juro Kodera : Dynamical Analysis of Reinforced Concrete Pier in Elasto-Plastic Range and its Application to Practical Design, Proceedings of JSCE,No.297,pp.71-85,May

1980.
[24] Tsuneo Miyatake and Toshiyuki Kubota : Study on Reinforced Concrete Columns I, Kanto Branch of ACJ, the 33th Annual Report, 1966.
[25] AIJ : Building Codes for Reinforced Concrete Structures.
[26] Japan Architectural Center : The State of the Arts on Preventing Collapse of Reinforced Concrete Columns, Concrete Journal Vol.13,No.1 pp.2-18, Jan. 1975.
[27] Clough, R. W. : Effect of Stiffness Degrading on Earthquake Ductility Requirement, Report 6614, Structural and Materials, Univ. of Calif., Berkeley, 1966.
[28] Yasuo Fukada : Hysteresis Loops of Reinforced Concrete Structures, Kanto Branch of AIJ, Nov. 1969.
[29] Takeda,T., Sozen. M. A. and Nielsen, N.N. : Reinforced concrete Response to Simulated Earthquake, Proc. of ASCE, Vol.96,ST.12,Dec.1970.